第 65 卷 第 10 期
2022 年 10 月

地 球 物 理 学 报
CHINESE JOURNAL OF GEOPHYSICS

Vol. 65, No. 10
Oct., 2022

王冠之,陈永顺,张晨等. 2022. 华南中部地幔转换带厚度异常:海南地幔柱? 地球物理学报,65(10):3871-3880,doi:10.6038/cjg2022P0338.

Wang G Z, Chen Y S, Zhang C, et al. 2022. Mantle transition zone thickness anomaly at middle Southern China by receiver function: evidence for Hainan Plume. *Chinese J. Geophys.* (in Chinese),65(10):3871-3880,doi:10.6038/cjg2022P0338.

华南中部地幔转换带厚度异常:海南地幔柱?

王冠之[1],陈永顺[2,3*],张晨[2],盖增喜[1],郭震[2,3],杨挺[2,3],葛天雨[1]

1 北京大学理论与应用地球物理研究所,北京 100871
2 南方科技大学海洋科学与工程系,广东深圳 518055
3 上海佘山地球物理国家野外科学观测研究站,上海 201602

摘要 本文利用 84 个布设于华南中部地区的流动地震台站记录的 239 个远震地震事件的波形资料,通过接收函数方法得到了华南大陆中部地区的地幔 410 km 和 660 km 间断面起伏与地幔转换带厚度变化.结果表明在华夏块体下方转换带厚度明显减薄 10~25 km,尤其是在南部靠近海岸线附近(23.7°N,114.5°E)存在一个直径约 200 km 的转换带厚度异常区域(减薄约 25 km),可能揭示海南地幔柱在该处上涌穿透 660 km 间断面进入地幔,在地幔转换带向周围扩散,热的地幔物质穿过 410 km 间断面继续上涌,造成了华夏块体下方上地幔大范围的低速异常,以及在雷州半岛和沿岸造成大范围的新生代玄武岩活动.

关键词 接收函数;410 km 间断面;660 km 间断面;转换带厚度;华夏块体;扬子克拉通

doi:10.6038/cjg2022P0338 **中图分类号** P315,P541 **收稿日期** 2021-05-18,2022-06-08 **收修定稿**

Mantle transition zone thickness anomaly at middle Southern China by receiver function: evidence for Hainan Plume

WANG GuanZhi[1], CHEN YongShun[2,3*], ZHANG Chen[2], GE ZengXi[1], GUO Zhen[2,3], YANG Ting[2,3], GE TianYu[1]

1 *Department of Geophysics, Peking University, Beijing* 100871, *China*
2 *Department of Ocean Science and Engineering, Southern University of Science and Technology, Guangdong Shenzhen* 518055, *China*
3 *ShanghaiSheshan National Geophysical Observatory, Shanghai* 201602, *China*

Abstract We have presented the 410 km and 660 km mantle discontinuity structure and mantle transition zone (MTZ) thickness beneath the middle Southern China Block using seismic data recorded by 84 portable seismic stations in the region by receiver function method. We found that transition zone thickness beneath Cathaysia Block is thinned 10~25 km obviously, the MTZ thinned anomalously within an area approximately 200 km in diameter centered (23.7°N,114.5°E), where the Hainan mantle plume may upwell into upper mantle,the continuous upwelling of hot mantle materials resulted in a wide range of low velocity anomalies in the upper mantle beneath the Cathaysia Block (above 410 km), also a large range of Cenozoic basalts in Leizhou Peninsula and coastal areas.

基金项目 国家自然科学基金项目(41890814,U1901602),大洋"十三五"项目(DY35-G2-1-01),广东省自然科学基金(2018A030310121),深圳市海外高层次人才创新创业专项资金团队资助项目(KQTD20170810111725321),中国地质科学院地质调查项目(DD20160082)资助.

第一作者简介 王冠之,男,1994 年生,硕士研究生,主要从事接收函数成像研究. E-mail:wanggz@pku.edu.cn

*通讯作者 陈永顺,男,教授,主要从事地震大地构造学和海洋地球物理学研究. E-mail:johnyc@sustech.edu.cn

Keywords Receiver function; 410 km discontinuity; 660 km discontinuity; Transition zone thickness; Cathaysia Block; Yangtze Craton

0 引言

中国华南大陆位于欧亚、印-澳、菲律宾海三大板块的交汇部位,自新元古代以来,该区发生了至少四期区域规模的地球动力学事件(舒良树,2012),其中,在显生宙期间经历了复杂的大陆俯冲及碰撞和岩浆侵入作用(Jahn et al., 1976; Seno and Maruyama, 1984; Briais et al., 1993; Hall et al., 1995; Okino et al., 1999; Gripp and Gordon, 2002; Huang et al. 2010; Li and Van Der Hilst, 2010; 张国伟等, 2013; 刘琼颖等,2013).现今的华南块体主要由扬子克拉通和华夏块体构成,二者大约于 0.88 Ga 时期碰撞(Li et al., 2009),在拼合处形成一条宽百余千米、延伸约 1300 km 的江南新元古代造山带.这两个块体在之后经历了不同的构造演化(Seno and Maruyama, 1984; Zhao and Cawood, 1999; Li Z X and Li X H, 2007; 舒良树,2012;张国伟等,2013).

近年来,随着数据的增加和精度的提高,一些地球物理观测研究表明,华南地区下方存在显著的地幔流活动(Jiang et al., 2015; Xia et al., 2016),相比于扬子克拉通,华夏块体发生了更加活跃的岩浆活动(Li, 2000; Zhou and Li, 2000),在华夏块体下方存在延伸至 400 km 深度的低速结构,而扬子克拉通下方则呈现明显的高速特征(Zhou and Li, 2000; Zheng et al., 2007; Chen and Pei, 2010; Gao et al.,2010; Zhao L et al., 2013; Jiang et al., 2013; Huang, 2014; Kusky et al., 2014; Shan et al., 2014; Zhao B et al., 2015; Sun et al., 2016;王晓冉等,2018;曲平等,2020).已有的走时层析成像结果由于分辨率等因素限制,对于地幔流的来源和形态尚存争议,对于华南块体下方的动力学机制,目前也没有统一的认识.

华南地区在新元古代时已经存在板块运动机制(Guo et al.,1989; Wang and Mo, 1995, Li et al., 1999),目前针对华南地区的地球动力学模型研究包括地幔上涌驱动的二阶地幔流(Deng et al., 2004)、俯冲带地幔楔环流(Niu et al., 2005; Maruyama et al., 2009)、俯冲平板破碎剥离引发地幔流动(Li Z X and Li X H, 2007)等多种,而对于地幔转换带结构的研究则为深部岩浆的存在范围和起源以及验证俯冲板片滞留提供了比较有力的证据(Ammon, 1991; Bina and Helffrich, 1994; Courtillot et al., 2003; Li et al., 2006, 2008).前人利用远震接收函数方法(Langston, 1979; Lawrence and Shearer, 2006)对华南东部地区、雷州半岛及其邻区进行了探索(Ai et al., 2007; Eagar et al., 2010; Gao et al., 2010; 王晨阳和黄金莉,2012;Li et al., 2013; 叶卓等, 2013,2014,2020; Huang et al., 2015; Wei and Chen, 2016; 张耀阳等,2018).但是,对于华南大陆中部地区,由于台站密度等原因,没有取得较高精度的结果.因此,本文基于最新布设的华南地区流动台阵的地震数据,利用远震接收函数的方法研究华南大陆中部地区上地幔间断面形态和转换带厚度变化,可以填补过去由于数据缺失所导致的深部地幔结构的盲区,为认识华南地区构造演化的动力学机制提供帮助和证据.

1 数据和方法

1.1 数据资料

本次研究采用北京大学及南方科技大学在 2016 年 12 月—2018 年 10 月布设于研究区域的 84 套宽频带流动地震台站记录的远震波形数据(图 1),并从震中距在 25°～95°之间的,震级大于 5.5 级的 673 个远震事件中挑选出 P 波初动清晰且信噪比较高的 239 个远震事件进行接收函数提取(图 2).所使用的流动地震仪(sensor)型号为 STS2.5 甚宽频地震计、3espc 及 3esp 宽频带地震计,流动地震观测仪配备的数据采集系统(DAS)型号为 REFTEK130 和 QuanterraQ330,仪器采样率设定为 100 Hz.

1.2 接收函数的提取

远震 P 波接收函数是远震波形的垂直分量与水平分量反褶积后得到的时间序列,根据 P 波入射到速度间断面时部分能量将转换成 S 波,利用转换震相波的出现判断存在速度间断面,利用转换震相与 P 波的到时差估计间断面的可能深度,从而避免了天然地震震源等因素的影响.本次研究中,从原始记录数据中截取 P 波初动前 10 s 到初动后 100 s 的地震波形,采用时间域迭代反褶积方法(Ligorría and Ammon, 1999),选取 2.5 的高斯滤波因子对接

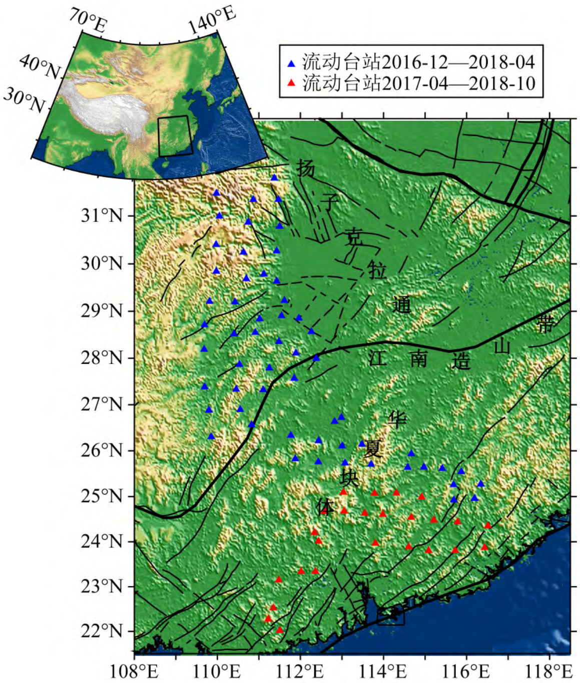

图 1　流动台站位置

黑色粗线(Zhang et al.，2003)为构造带位置，黑色细线为断层位置.

Fig. 1　Position of portable seismic stations

The black thick lines (Zhang et al.，2003) show the position of tectonic belts，the black thin lines show the position of faults.

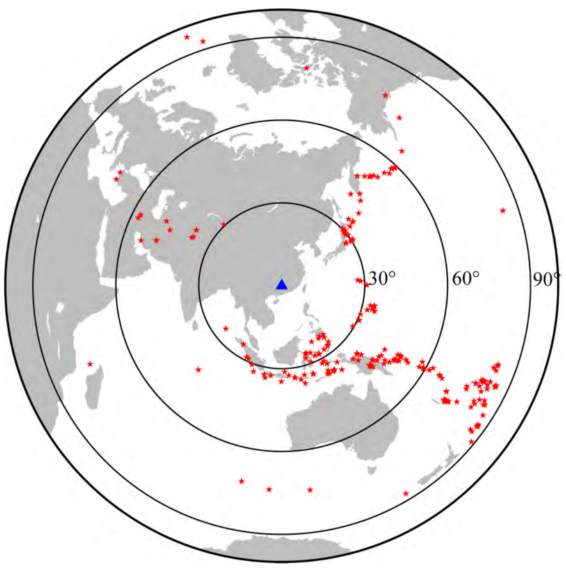

图 2　研究使用远震事件分布

蓝色三角形显示研究区域中心位置，红星为远震事件.

Fig. 2　Maps of teleseismic events used in the study

The blue triangle illustrates the central position of research area，red stars represent teleseismic events.

收函数进行滤波，取迭代次数为 100 计算提取 P 波接收函数，然后对得到的接收函数进行人工挑选，选取初动及转换波震相清晰、信噪比高的接收函数 2172 条. 图 3 以 BD19 台为例给出了信噪比较高的接收函数波形.

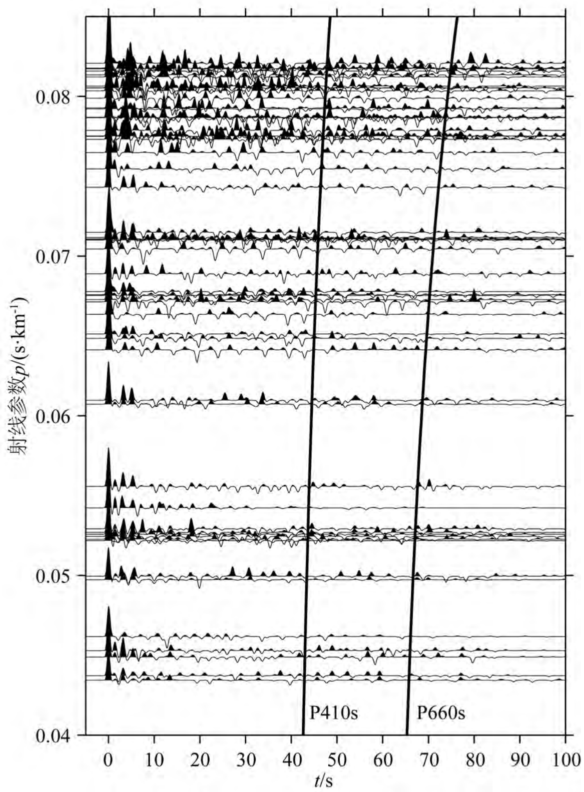

图 3　BD19 台全部接收函数

两条黑色曲线分别代表由 IASP91 模型计算得到的 P410s 和 P660s 参考到时.

Fig. 3　Receiver functions of BD19 station

The two black lines show the reference time of P410s & P660s calculated with IASP91 model.

实际地震波记录由于噪声的影响，地幔转换带两个间断面转换波震相不清晰，为了加强转换波信号，减弱随机干扰的影响，本研究采用共面元叠加的方法对挑选得到的接收函数进行叠加. 将所得到的原始接收函数以参考震中距 56°进行时差校正，从而消除震中距不同对转换波到时的影响；然后计算接收函数射线在不同深度入射点在地表的投影位置，并将入射点位于同一面元的接收函数进行聚束叠加(Hedlin et al.，1991；Zhu and Kanamori，2000)，叠加后接收函数在 410 km 和 660 km 的转换波得到加强. 鉴于本文着重于对地幔转换带的研究，周期为 5 s 的地震波在 410 km 和 660 km 深度的菲涅尔带半径大约为 150 km，综合考虑间断面深度和信号的主周期，将面元设计为边长 150 km 的正方形，水平方向上面元移动步长为 50 km，垂直方向上面元间距为 10 km.

2 结果

应用IASP91模型将叠加后的接收函数由时间域转换至深度域,得到研究区域下方410 km和660 km间断面的结构和转换带厚度.图4展示了4个接收函数叠加深度剖面,下方为相应的时间域剖面,图5a中展示了这4个剖面位置.

深度剖面L1中,410 km间断面(红色)深度在400～430 km范围内变化且由南至北呈现"由深到浅"连续过渡,间断面在28°N—29°N的位置起伏明显:在23.5°N至28°N之间为420～430 km,24.5°N附近最深至430 km;自29°N至32°N,410 km逐渐抬升至400 km.660 km间断面(红色)深度在660～680 km范围内变化:25°N—29°N变化平缓,其深度分布在660 km附近,自25°N至23°N,该间断面深度沉降至680 km;从29°N—32°N深度又由660 km逐渐沉降到678 km.

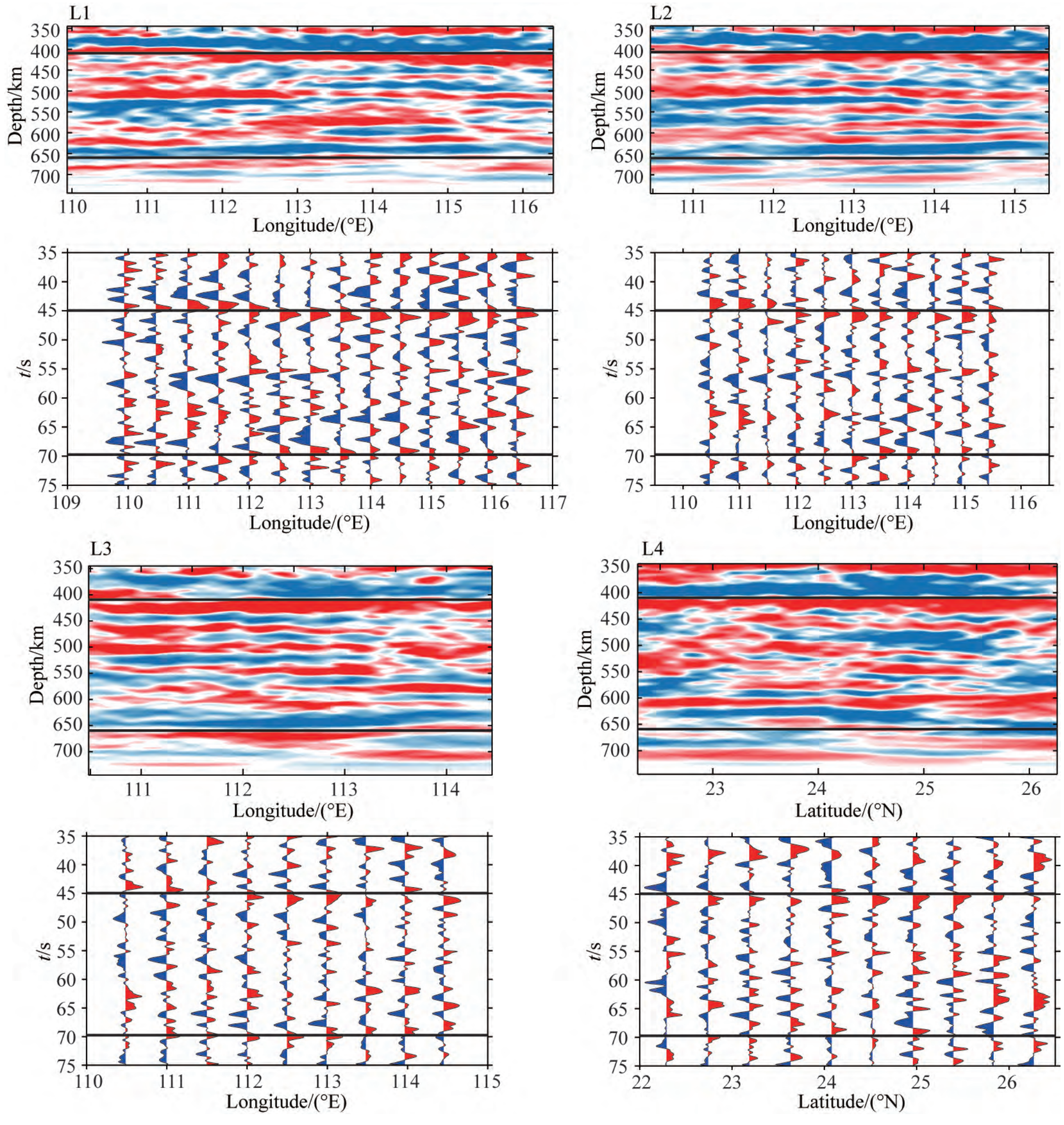

图4 接收函数叠加剖面图

黑色实线分别为P410s和P660s在时间域剖面参考到时,并在深度域剖面标出了410 km和660 km深度位置,红色和蓝色分别代表波峰的正负.整体而言,华夏块体下方410 km间断面下沉5～10 km,660 km间断面整体下沉但偏离模型较小,660 km间断面在(23.7°N,114.5°E)位置有10～15 km抬升.

Fig.4 Stack of receiver function profiles

The black lines show the reference time of P410s and P660s in time domain, which also mark the depth of 410 km and 660 km in depth domain. Red and blue colors represent positive and negative phase. The 410 km discontinuity beneath the Cathaysia Block sank by 5～10 km, the 660 km discontinuity sank totally, but the deviation from the model was small, and the 660 km discontinuity lifted by 10～15 km at (23.7°N, 114.5°E).

深度剖面 L2 中，410 km 间断面（红色）深度变化与 L1 中变化相似，但其深度整体上在 400 km 至 422 km 内变化：23°N—27°N 间断面深度变化平缓，沉降至 420 km 附近，27°N—29°N 深度由 410 km 逐渐抬升至 400 km；23°N—26.5°N 内 660 km（红色）间断面深度在 660 km 附近变化，26.5°N—29°N 内其深度逐渐沉降至 675 km.

剖面 L3 中，410 km 间断面（红色）整体下沉并在 420 km 附近变化，另外，在 27°N 以北还存在局部分层现象，660 km 间断面（红色）整体变化也比较平缓，23°N 附近抬升至 650 km 附近，24°N—27°N 略有沉降，但都接近全球平均.

L4 剖面 410 km 间断面（红色）整体下沉，23.5°N—24°N 达 420 km，25°N—26°N 达到 425 km，660 km 间断

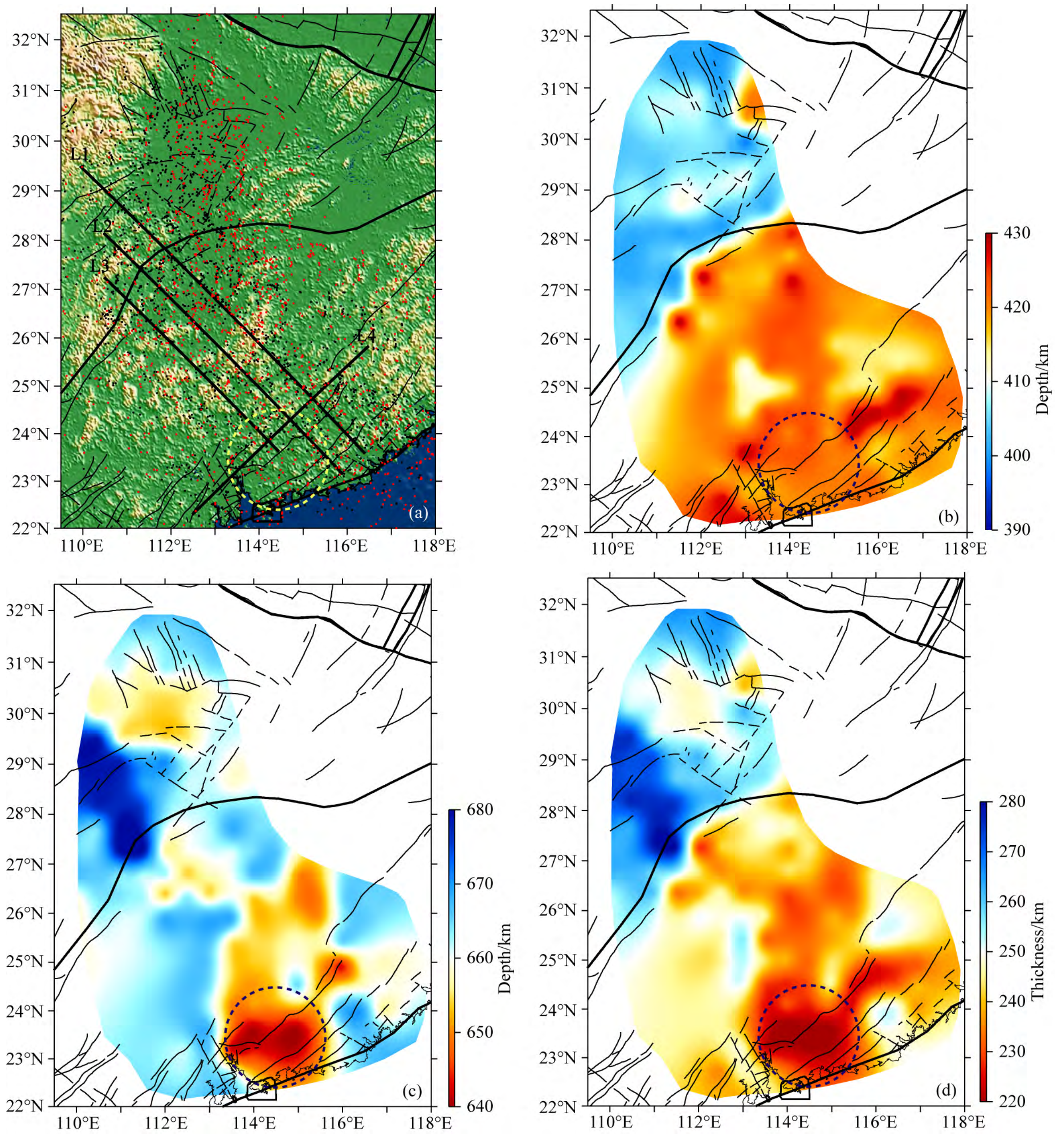

图 5　410 km、660 km 间断面深度及地幔转换带厚度分布

（a）研究区域剖面位置，黑色和红色的点分别为 410 km 和 660 km 间断面转换点位置；（b）410 km 间断面深度分布；（c）660 km 间断面深度分布；（d）研究区域地幔转换带厚度分布. 图中虚线圆表示地幔柱可能的位置.

Fig. 5　Maps of 410 km, 660 km discontinuity's depth and thickness of mantle transition zone

(a) Position of profiles in research area, black and red points show the position of piercing point at 410 km & 660 km discontinuity; (b) The 410 km discontinuity depth map; (c) The 660 km discontinuity depth map; (d) Mantle transition zone thickness map beneath research area. The dotted circle shows the possible position of plume.

面(红色)在23.5°N—24°N抬升至645 km附近,25°N—27°N整体沉降至670 km附近.

对各个面元分别进行计算并插值分别得到这两个间断面空间分布(图5).结果显示,以扬子地块和华夏地块的分界线为界,两边的地幔转换带结构显示出巨大差别:在研究区域以南的华夏地块下方,410 km间断面较IASP91速度模型深,660 km间断面较IASP91速度模型在(23.7°N,114.5°E)位置有10～15 km抬升,其余地区整体下沉但偏离模型较小;北部的扬子地块410 km间断面深度较IASP91速度模型略有抬升,而660 km间断面在(27.5°N,111°E)地区下沉到680 km.将两间断面深度绝对值相减得到转换带厚度分布(图5d),结果显示华夏地块下方的地幔转换带厚度约225～250 km,最显著的特征是在(23.7°N,114.5°E)位置存在一个直径约200 km的转换带厚度异常薄区域,其厚度约225 km;扬子地块下方的地幔转换带厚度为248～275 km,在27.5°N—29°N有一个带状异常增厚区,该区域南北长度约150 km,其厚度约275 km.需要指出,上述结果没有考虑速度横向变化的影响,因此无法确定地幔转换带的差异是由于扬子地块与华夏地块的物质组成差异引起的,还是由速度模型偏离实际速度分布引起的.

3 讨论

目前普遍认为,地幔转换带厚度的变化与温度有关.高温高压矿物学实验表明:410 km间断面为α相橄榄石到β相尖晶石的相变面,而660 km间断面为γ相尖晶石到钙钛矿加方镁铁矿的相变面,两间断面处的物理相变过程具有相反的克拉伯龙斜率(Weidner and Wang, 1998),温度的增加会使410 km间断面下降和660 km间断面抬升,导致转换带厚度减薄,反之温度的降低则使转换带厚度增加(Bina and Helffrich, 1994; Lebedev et al., 2003).本文研究结果(图5b)显示410 km间断面深度较全球一维速度模型(IASP91)在江南造山带以南的华夏块体内有明显大范围的下沉,在以北的扬子克拉通内部略有抬升,这说明在华夏块体下方的地幔转换带顶部410 km深度附近可能存在温度较高的地幔物质.

根据660 km间断面深度分布(图5c)可以看出,在华夏块体的中南部沿海地区该间断面明显抬升10～15 km.660 km间断面的抬升主要集中在深圳以北、以(23.7°N,114.5°E)为中心、半径为100 km的范围内(图5c黑色点划线圆).一种可能的解释是这里可能存在地幔柱上涌,下地幔物质从该处上涌进入地幔转换带,并在转换带内向周围扩散,进而导致华夏块体下方410 km间断面大范围的下沉(高温异常).

有关海南地幔柱的存在与否一直是学术界争议的热门话题,本文有关华夏块体下方地幔转换带厚度变化的观测结果支持海南地幔柱的存在.根据本文410 km间断面和660 km间断面深度分布结果(图5),我们认为来自下地幔的海南地幔柱(直径约200 km)在深圳以北(23.7°N,114.5°E)位置上涌穿过660 km间断面进入地幔转换带(Hirose, 2002),然后在地幔转换带内上涌的同时向周围扩散,导致华夏块体下方410 km间断面深度在较大范围内下沉(温度增加而深度变深)(图6),热的地幔物质继续上涌造成了华夏块体下方、410 km以上的上地幔大范围的低速异常(曲平等,2020),最终导致了雷州半岛以及沿岸大范围的新生代玄武岩活动(Zou and Fan, 2010; Wei and Chen, 2016).

由于地幔转换带以上的上地幔速度横向变化可能会同时影响410 km和660 km这两个间断面的

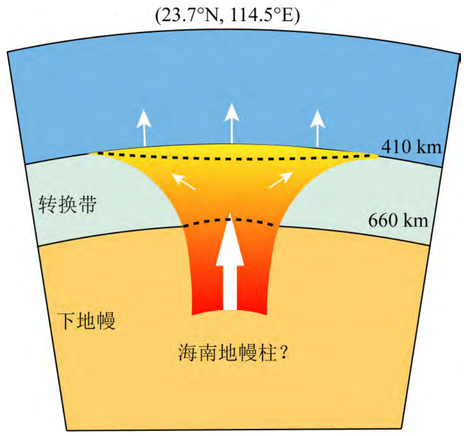

图6 海南地幔柱上涌示意图

来自下地幔的海南地幔柱(直径约200 km)中心在深圳以北(23.7°N, 114.5°E)位置上涌穿过660 km间断面进入地幔转换带,造成该处的660 km间断面隆升,然后在地幔转换带内继续上涌并向周围扩散,导致相对应的410 km间断面在较大范围内因为升温下沉.

Fig.6 Diagram of Hainan mantle plume upwelling

The ascending Hainan mantle plume from lower mantle (about 200 km in diameter) passed through the 660 km discontinuity at north of Shenzhen (23.7°N, 114.5°E), caused the uplift of 660 km discontinuity and entered into the mantle transition zone. It then surged up and expanded laterally in the mantle transition zone, resulting in the subsidence of the 410 km discontinuity with the elevated temperature.

绝对深度,而转换带内部横向非均匀性相对较小,因此,在不考虑上地幔速度横向变化影响的情况下,地幔转换带厚度的变化特征更能反映出转换带(温度)结构.在华夏块体下方(23.7°N,114.5°E)位置存在约25 km的转换带减薄,若只考虑温度对转换带厚度的影响,则相当于大约 250 K 的局部温度上升(Helffrich,2000;Kumagai et al.,2007),对应于 P 波速度存在 1.1%的低速异常(Cammarano et al.,2003),这与前人在该区域得到的体波层析成像和接收函数结果基本一致(Lebedev and Nolet,2003;Courtillot V et al.,2003;Montelli et al.,2004;Li and Van Der Hilst,2010;Wei et al.,2012;Schaeffer and Lebedev,2013;Huang et al.,2015;Sun et al.,2016;Wei and Chen,2016;曲平等,2020).体波层析成像结果表明在华夏块体下方的地幔转换带内,存在比较强的低速异常体,且南部靠近海岸线最强,逐渐向北减弱,暗示华夏块体下方的低速异常可能来源于南部靠近海岸线处下地幔的上升热地幔物质流(Hsu et al.,2004;夏少红等,2007;Lei et al.,2009;Xia et al.,2010;Jiang et al.,2015;Xia et al.,2016;Liu et al.,2017;曲平等,2020),并进一步暗示此处可能存在地幔柱.

另一方面,针对于广东、广西及海南地区的 SKS 横波分裂研究结果表明(葛天雨等,2022),在深圳以北的地区存在较多的 null 值结果(图 7)(当快轴偏振方向与入射方向一致时,这时的结果将会是 null 值)说明该处的地幔流向可能沿垂向,也为该处可能存在地幔柱提供了有力的证据.

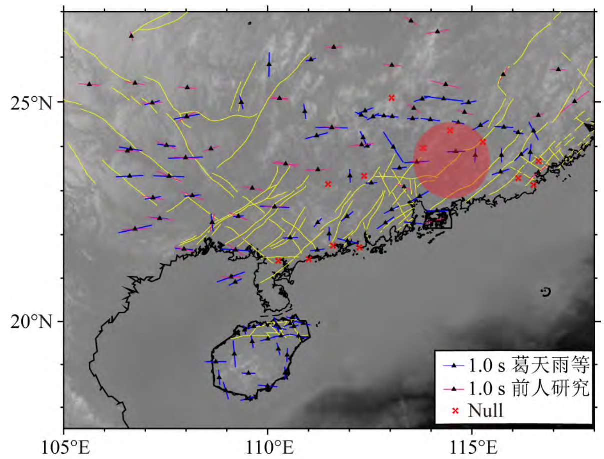

图 7　SKS 横波分裂结果图(葛天雨等,2022)

图中黑色三角形代表台站位置,蓝色及粉色短线的长短表示延迟时间,方向表示快轴偏振方向,红叉表示 null 值,红色圆圈表示地幔柱可能的位置.从横波分裂结果来看,在深圳以北地区存在较多 null 值,暗示此处可能存在地幔柱.

Fig.7　Diagram of SKS shear wave splitting result (Ge et al.,2022)

Black triangles in the figure represent the station position, the lengths of blue and pink lines indicate the delay time, the direction shows the fast axis polarization direction, the red "×" indicates null value, and the red circle shows the possible position of plume. From the results of shear wave splitting, there are many null values in the north of Shenzhen, suggesting that there may be mantle plume.

4　结论

本文利用 84 个流动地震台站的远震地震波形记录,通过接收函数的方法得到了华南大陆中部地区的 410 km 和 660 km 间断面分布与地幔转换带厚度变化.结果表明在华夏块体中南部下方地幔转换带厚度明显减薄 10～25 km,这与近年来地震层析成像和地球化学在华夏块体的研究结果相一致,尤其是主要集中在南部靠近海岸线附近以(23.7°N,114.5°E)为中心、直径为 200 km 的范围内,可能是海南地幔柱在该处上涌进入上地幔,在地幔转换带向周围扩散,热地幔物质流穿过 410 km 间断面继续上涌造成了华夏块体下方上地幔大范围的低速异常,最终导致了雷州半岛和沿岸大范围的新生代玄武岩活动.

致谢　感谢北京大学冯永革高级工程师和南方科技大学邹长桥工程师带领的流动台站野外工作组所有成员的辛勤付出.数据处理和绘图使用到 SAC (Seismic Analysis Code)和 GMT5(Wessel and Smith,1998)软件.

References

Ai Y S, Chen Q F, Zeng F, et al. 2007. The crust and upper mantle structure beneath southeastern China. *Earth and Planetary Science Letters*, 260(3-4): 549-563.

Ammon G J. 1991. The isolation of receiver effects fromteleseismic P waveforms. *Bulletin of the Seismological Society of America*, 81(6): 2504-2510.

Bina C R, Helffrich G. 1994. Phase transition Clapeyron slopes and transition zone seismic discontinuity topography. *Journal of Geophysical Research: Solid Earth*, 99(B8): 15853-15860.

Briais A, Patriat P, Tapponnier P. 1993. Updated interpretation of magnetic anomalies and seafloor spreading stages in the South China Sea: Implications for the Tertiary tectonics of Southeast Asia. *Journal of Geophysical Research: Solid Earth*, 98(B4): 6299-6328.

Cammarano F, Goes S, Vacher P, et al. 2003. Inferring upper-mantle temperatures from seismic velocities. *Physics of the Earth and Planetary Interiors*, 138(3-4): 197-222, doi: 10.1016/S0031-9201(03)00156-0.

Chen Y J, Pei S P. 2010. Tomographic structure of East Asia: Ⅱ. Stagnant slab above 660 km discontinuity and its geodynamic implications. *Earthquake Science*, 23(6): 613-626.

Courtillot V, Davaille A, Besse J, et al. 2003. Three distinct types of hotspots in the Earth's mantle. *Earth and Planetary Science Letters*, 205(3-4): 295-308.

Deng J F, Mo X X, Zhao H L, et al. 2004. A new model for the dynamic evolution of Chinese lithosphere: 'continental roots-plume tectonics'. *Earth-Science Reviews*, 65(3-4):223-275.

Eagar K C, Fouch M J, James D E. 2010. Receiver function imaging of upper mantle complexity beneath the Pacific Northwest, United States. *Earth and Planetary Science Letters*, 297(1-2): 141-153.

Gao Y A, Suetsugu D, Fukao Y, et al. 2010. Seismic discontinuities in the mantle transition zone and at the top of the lower mantle beneath eastern China and Korea: Influence of the stagnant Pacific slab. *Physics of the Earth and Planetary Interiors*, 183(1-2): 288-295.

Ge T Y, Chen Y S, Zhang C. 2022. Study of Hainan mantle plume based on shear wave splitting method. *Acta Scientiarum Naturalium Universitatis Pekinensis* (in Chinese), 2022, 58(2): 261-270.

Gripp A E, Gordon R G. 2002. Young tracks of hotspots and current plate velocities. *Geophysical Journal International*, 150(2):321-361.

Guo L Z, Shi Y S, Lu H F, et al. 1989. The pre-Devonian tectonic patterns and evolution of South China. *Journal of Southeast Asian Earth Sciences*, 3(1): 87-93.

Hall R, Ali J R, Anderson C D, et al. 1995. Origin and motion history of the Philippine Sea Plate. *Tectonophysics*, 251(1-4): 229-250.

Hedlin M A H, Minster J B, Orcutt J A. 1991. Beam-stack imaging using a small aperture array. *Geophysical Research Letters*, 18(9): 1771-1774.

Helffrich G. 2000. Topography of the transition zone seismic discontinuities. *Reviews of Geophysics*, 38(1): 141-158.

Hirose K. 2002. Phase transitions inpyrolitic mantle around 670-km depth: Implications for upwelling of plumes from the lower mantle. *Journal of Geophysical Research: Solid Earth*, 107(B4): ECV 3-1-ECV 3-13, doi: 10.1029/2001JB000597.

Hsu S K, Yeh Y C, Doo W B, et al. 2004. New bathymetry and magnetic lineations identifications in the northernmost South China Sea and their tectonic implications. *Marine Geophysical Researches*, 25(1): 29-44.

Huang H B, Tosi N, Chang S J, et al. 2015. Receiver function imaging of the mantle transition zone beneath the South China Block. *Geochemistry, Geophysics, Geosystems*, 16(10): 3666-3678, doi: 10.1002/2015GC005978.

Huang J L. 2014. P-and S-wave tomography of the Hainan and surrounding regions: Insight into the Hainan plume. *Tectonophysics*, 633: 176-192.

Huang Z C, Wang L S, Zhao D P, et al. 2010. Upper mantle structure and dynamics beneath Southeast China. *Physics of the Earth and Planetary Interiors*, 182(3-4): 161-169.

Jahn B M, Chen P Y, Yen T P. 1976. Rb-Sr ages of granitic rocks in Southeastern China and their tectonic significance. *GSA Bulletin*, 87(5): 763-776.

Jiang G M, Zhang G B, Lü Q T, et al. 2013. 3-D velocity model beneath the Middle-Lower Yangtze River and its implication to the deep geodynamics. *Tectonophysics*, 606: 36-47.

Jiang G M, Zhang G B, Zhao D P, et al. 2015. Mantle Dynamics and Cretaceousmagmatism in east-central China: Insight from teleseismic tomograms. *Tectonophysics*, 664: 256-268.

Kumagai I, Davaille A, Kurita K. 2007. On the fate of thermally buoyant mantle plumes at density interfaces. *Earth and Planetary Science Letters*, 254(1-2): 180-193, doi: 10.1016/j.epsl.2006.11.029.

Kusky T M, Windley B F, Wang L, et al. 2014. Flat slab subduction, trench suction, and craton destruction: comparison of the North China, Wyoming, and Brazilian cratons. *Tectonophysics*, 630: 208-221.

Langston C A. 1979. Structure under Mount Rainier, Washington, inferred from teleseismic body waves. *Journal of Geophysical Research: Solid Earth*, 84(B9): 4749-4762.

Lawrence J F, Shearer P M. 2006. A global study of transition zone thickness using receiver functions. *Journal of Geophysical Research: Solid Earth*, 111(B6): B06307, doi: 10.1029/2005JB003973.

Lebedev S, Chevrot S, Van Der Hilst R D. 2003. Correlation between the shear-speed structure and thickness of the mantle transition zone. *Physics of the Earth and Planetary Interiors*, 136(1-2): 25-40.

Lebedev S, Nolet G. 2003. Upper mantle beneath Southeast Asia from *S* velocity tomography. *Journal of Geophysical Research: Solid Earth*, 108(B1): 2048, doi: 10.1029/2000JB000073.

Lei J S, Zhao D P, Steinberger B, et al. 2009. New seismic constraints on the upper mantle structure of the Hainan plume. *Physics of the Earth and Planetary Interiors*, 173(1-2): 33-50.

Li C, Van Der Hilst R D, Toksöz M N. 2006. Constraining *P*-wave velocity variations in the upper mantle beneath Southeast Asia. *Physics of the Earth and Planetary Interiors*, 154(2): 180-195.

Li C, Van Der Hilst R D, Meltzer A S, et al. 2008. Subduction of the Indian lithosphere beneath the Tibetan plateau and Burma. *Earth and Planetary Science Letters*, 274(1-2): 157-168.

Li C, Van DerHilst R D. 2010. Structure of the upper mantle and transition zone beneath Southeast Asia from traveltime tomography. *Journal of Geophysical Research: Solid Earth*, 115(B7): B07308, doi: 10.1029/2009JB006882.

Li Q S, Gao R, Wu F T, et al. 2013. Seismic structure in the southeastern China using teleseismic receiver functions. *Tectonophysics*, 606: 24-35.

Li X H. 2000. Cretaceous magmatism and lithospheric extension in Southeast China. *Journal of Asian Earth Sciences*, 18(3): 293-305.

Li X H, Li W X, Li Z X, et al. 2009. Amalgamation between the Yangtze andCathaysia Blocks in South China: constraints from SHRIMP U-Pb zircon ages, geochemistry and Nd-Hf isotopes of the Shuangxiwu volcanic rocks. *Precambrian Research*, 174

(1-2): 117-128.

Li Z X, Li X H, Kinny P D, et al. 1999. The breakup of Rodinia: Did it start with a mantle plume beneath South China? *Earth and Planetary Science Letters*, 173(3): 171-181.

Li Z X, Li X H. 2007. Formation of the 1300-km-wide intracontinental orogen and postorogenic magmatic province in Mesozoic South China: a flat-slab subduction model. *Geology*, 35(2): 179-182.

Ligorría J P, Ammon C J. 1999. Iterative deconvolution and receiver-function estimation. *Bulletin of the Seismological Society of America*, 89(5): 1395-1400.

Liu Q Y, He L J, Huang F. 2013. Review of Mesozoic geodynamics research of South China. *Progress in Geophysics* (in Chinese), 28(2): 633-647, doi: 6038/pg20130212.

Liu X, Zhao D P, Li S Z, et al. 2017. Age of the subducting Pacific slab beneath East Asia and its geodynamic implications. *Earth and Planetary Science Letters*, 464: 166-174.

Maruyama S, Hasegawa A, Santosh M, et al. 2009. The dynamics of big mantle wedge, magma factory, and metamorphic-metasomatic factory in subduction zones. *Gondwana Research*, 16(3-4): 414-430.

Montelli R, Nolet G, Dahlen F A, et al. 2004. Finite-frequency tomography reveals a variety of plumes in the mantle. *Science*, 303(5656): 338-343.

Niu Z J, Wang M, Sun H R, et al. 2005. Contemporary velocity field of crustal movement of Chinese mainland from global positioning system measurements. *Chinese Science Bulletin*, 50(9): 939-941.

Okino K, Ohara Y, Kasuga S, et al. 1999. The Philippine Sea: New survey results reveal the structure and the history of the marginal basins. *Geophysical Research Letters*, 26(15): 2287-2290.

Qu P, Chen Y S, Yu Y, et al. 2020. 3D velocity structure of upper mantle beneath South China and its tectonic implications: evidence from finite frequency seismic tomography. *Chinese Journal of Geophysics* (in Chinese), 63(8): 2954-2969, doi: 10.6038/cjg2020N0183.

Schaeffer A J, Lebedev S. 2013. Global shear speed structure of the upper mantle and transition zone. *Geophysical Journal International*, 194(1): 417-449.

Seno T, Maruyama S. 1984. Paleogeographic reconstruction and origin of the Philippine Sea. *Tectonophysics*, 102(1-4): 53-84.

Shan B, Afonso J C, Yang Y J, et al. 2014. The thermochemical structure of the lithosphere and upper mantle beneath South China: Results from multiobservable probabilistic inversion. *Journal of Geophysical Research: Solid Earth*, 119(11): 8417-8441, doi: 10.1002/2014JB011412.

Shu L S. 2012. An analysis of principal features of tectonic evolution in South China Block. *Geological Bulletin of China* (in Chinese), 31(7): 1035-1053, doi: 10.3969/j.issn.1671-2552.2012.07.003.

Sun Y, Liu J X, Tang Y C, et al. 2016. Structure of the upper mantle and transition zone beneath the South China block imaged by finite frequency tomography. *Acta Geological Sinica (English Edition)*, 90(5): 1637-1652.

Wang C Y, Huang J L. 2012. Mantle transition zone structure around Hainan by receiver function analysis. *Chinese Journal of Geophysics* (in Chinese), 55(4): 1161-1167, doi: 10.6038/j.issn.0001-5733.2012.04.012.

Wang X R, Li Q S, Zhang H S, et al. 2018. Study of P-wave velocity structure in upper mantle in eastern South China. *Global Geology* (in Chinese), 37(2): 620-626, doi: 10.3969/j.issn.1004-5589.2018.02.029.

Wang H Z, Mo X X. 1995. An outline if the tectonic evolution of China. *Episodes*, 18(1-2): 6-16.

Wei S S, Chen Y J. 2016. Seismic evidence of the Hainan mantle plume by receiver function analysis in southern China. *Geophysical Research Letters*, 43(17): 8978-8985, doi: 10.1002/22016GRL069513.

Wei W, Xu J D, Zhao D P, et al. 2012. East Asia mantle tomography: New insight into plate subduction and intraplate volcanism. *Journal of Asian Earth Sciences*, 60: 88-103.

Weidner D J, Wang Y B. 1998. Chemical- and Clapeyron-induced buoyancy at the 660 km discontinuity. *Journal of Geophysical Research: Solid Earth*, 103(B4): 7431-7441.

Wessel P, Smith W H F. 1998. New, improved version of Generic Mapping Tools released. *Eos, Transactions American Geophysical Union*, 79(47): 579.

Xia S H, Qiu X L, Zhao M H, et al. 2007. Data processing of onshore-offshore seismic experiment in Hongkong and Zhujiang River Delta region. *Journal of Tropical Oceanography* (in Chinese), 26(1): 35-38, doi: 10.3969/j.issn.1009-5470.2007.01.006.

Xia S H, Zhao M H, Qiu X L, et al. 2010. Crustal structure in an onshore-offshore transitional zone near Hong Kong, northern South China Sea. *Journal of Asian Earth Sciences*, 37(5-6): 460-472.

Xia S H, Zhao D P, Sun J L, et al. 2016. Teleseismic imaging of the mantle beneath southernmost China: New insights into the Hainan plume. *Gondwana Research*, 36: 46-56.

Ye Z, Li Q S, Gao R, et al. 2013. Seismic receiver functions revealing crust and upper mantle structure beneath the continental margin of southeastern China. *Chinese Journal of Geophysics* (in Chinese), 56(9): 2947-2958, doi: 10.6038/cjg20130909.

Ye Z, Li Q S, Gao R, et al. 2014. A thinned lithosphere beneath coastal area of southeastern China as evidenced by seismic receiver functions. *Science China Earth Sciences*, 57(11): 2835-2844, doi: 10.1007/s11430-014-4863-y.

Ye Z, Li Q S, Zhang H S, et al. 2020. A seismic receiver function study for the crustal and upper mantle structures of the Lower Yangtze and adjacent areas and its geological implications. *Acta Geologica Sinica* (in Chinese), 2020, 94(3): 707-715, doi: 10.3969/j.issn.0001-5717.2020.03.003.

Zhang G W, Guo A L, Wang Y J, et al. 2013. Tectonics of South China continent and its implications. *Science China Earth Sciences*, 56(11): 1804-1828, doi: 10.1007/s11430-013-4679-1.

Zhang P, Deng Q, Zhang G, et al. 2003. Active tectonic blocks and strong earthquakes in the continent of China. *Science in China Series D: Earth Sciences*, 46(2): 13-24.

Zhang Y Y, Chen L, Ai Y S, et al. 2018. Lithospheric structure of the South China Block from S-receiver function. *Chinese Journal of Geophysics* (in Chinese), 61(1): 138-149, doi: 10.6038/cjg2018L0226.

Zhao B, Huang Y, Zhang C H, et al. 2015. Crustal deformation on the Chinese mainland during 1998-2014 based on GPS data. *Geodesy and Geodynamics*, 6(1):7-15.

Zhao G C, Cawood P A. 1999. Tectonothermal evolution of the Mayuan assemblage in the Cathaysia Block: Implications for Neoproterozoic collision-related assembly of the South China craton. *American Journal of Science*, 299(4): 309-339.

Zhao L, Zheng T Y, Lu G. 2013. Distinct upper mantle deformation of cratons in response to subduction: constraints from SKS wave splitting measurements in eastern China. *Gondwana Research*, 23(1):39-53.

Zheng Y F, Zhang S B, Zhao Z F, et al. 2007. Contrasting zircon Hf and O isotopes in the two episodes of Neoproterozoic granitoids in South China: implications for growth and reworking of continental crust. *Lithos*, 96(1-2):127-150.

Zhou X M, Li W X. 2000. Origin of Late Mesozoic igneous rocks in Southeastern China: Implications for lithosphere subduction and underplating of mafic magmas. *Tectonophysics*, 326(3-4): 269-287.

Zhu L P, Kanamori H. 2000. Moho depth variation in southern California from teleseismic receiver functions. *Journal of Geophysical Research: Solid Earth*, 105(B2): 2969-2980.

Zou H B, Fan Q C. 2010. U-Th isotopes in Hainan basalts: Implications for sub-asthenospheric origin of EM2 mantle endmember and the dynamics of melting beneath Hainan Island. *Lithos*, 116(1-2): 145-152.

附中文参考文献

葛天雨，陈永顺，张晨. 2022. **基于横波分裂方法的海南地幔柱研究. 北京大学学报:自然科学版**, 2022, 58(2): 261-270.

刘琼颖，何丽娟，黄方. 2013. **华南中生代地球动力学机制研究进展. 地球物理学进展**, 28(2): 633-647, doi: 6038/pg20130212.

曲平，陈永顺，于勇等. 2020. **华南地区上地幔P波三维速度结构和动力学意义：来自有限频层析成像的证据. 地球物理学报**, 63(8): 2954-2969, doi: 10.6038/cjg2020N0183.

舒良树. 2012. **华南构造演化的基本特征. 地质通报**, 31(7): 1035-1053, doi: 10.3969/j.issn.1671-2552.2012.07.003.

王晨阳，黄金莉. 2012. **应用接收函数方法研究海南及其邻区地幔转换带结构. 地球物理学报**, 55(4): 1161-1167, doi: 10.6038/j.issn.0001-5733.2012.04.012.

王晓冉，李秋生，张洪双等. 2018. **华南东部地区上地幔P波速度结构研究. 世界地质**, 37(2): 620-626, doi: 10.3969/j.issn.1004-5589.2018.02.029.

夏少红，丘学林，赵明辉等. 2007. **香港与珠三角地区海陆联合地震探测的数据处理. 热带海洋学报**, 26(1): 35-38, doi: 10.3969/j.issn.1009-5470.2007.01.006.

叶卓，李秋生，高锐等. 2013. **中国大陆东南缘地震接收函数与地壳和上地幔结构. 地球物理学报**, 56(9): 2947-2958, doi: 10.6038/cjg20130909.

叶卓，李秋生，高锐等. 2014. **中国东南沿海岩石圈减薄的地震接收函数证据. 中国科学：地球科学**, 44(1): 2451-2460, doi: 10.1007/s11430-014-4863-y.

叶卓，李秋生，张宏双等. 2020. **下扬子及其邻区地壳和上地幔结构的接收函数研究及其地质意义. 地质学报**, 2020, 94(3): 707-715, doi: 10.3969/j.issn.0001-5717.2020.03.003.

张国伟，郭安林，王岳军等. 2013. **中国华南大陆构造与问题. 中国科学：地球科学**, 43(10): 1553-1582.

张耀阳，陈凌，艾印双等. 2018. **利用S波接收函数研究华南块体的岩石圈结构. 地球物理学报**, 61(1): 138-149, doi: 10.6038/cjg2018L0226.

（本文编辑　何燕）